Palmitoylation influences the function and pharmacology of sodium channels

Frank Bosmans[1], Mirela Milescu, and Kenton J. Swartz[1]

Molecular Physiology and Biophysics Section, Porter Neuroscience Research Center, National Institute of Neurological Disorders and Stroke, National Institutes of Health, Bethesda, MD 20892

Edited by William A. Catterall, University of Washington School of Medicine, Seattle, WA, and approved October 31, 2011 (received for review May 26, 2011)

Palmitoylation is a common lipid modification known to regulate the functional properties of various proteins and is a vital step in the biosynthesis of voltage-activated sodium (Nav) channels. We discovered a mutation in an intracellular loop of rNav1.2a (G1079C), which results in a higher apparent affinity for externally applied PaurTx3 and ProTx-II, two voltage sensor toxins isolated from tarantula venom. To explore whether palmitoylation of the introduced cysteine underlies this observation, we compared channel susceptibility to a range of animal toxins in the absence and presence of 2-Br-palmitate, a palmitate analog that prevents palmitate incorporation into proteins, and found that palmitoylation contributes to the increased affinity of PaurTx3 and ProTx-II for G1079C. Further investigations with 2-Br-palmitate revealed that palmitoylation can regulate the gating and pharmacology of wild-type (wt) rNav1.2a. To identify rNav1.2a palmitoylation sites contributing to these phenomena, we substituted three endogenous cysteines predicted to be palmitoylated and found that the gating behavior of this triple cysteine mutant is similar to wt rNav1.2a treated with 2-Br-palmitate. As with chemically depalmitoylated rNav1.2a channels, this mutant also exhibits an increased susceptibility for PaurTx3. Additional mutagenesis experiments showed that palmitoylation of one cysteine in particular (C1182) primarily influences PaurTx3 sensitivity and may enhance the inactivation process of wt rNav1.2a. Overall, our results demonstrate that lipid modifications are capable of altering the gating and pharmacological properties of rNav1.2a.

cholesterol | lipid microdomains | sphingomyelin

Because of their essential role in generating and propagating action potentials in excitable tissues (1–3), voltage-activated sodium (Nav) channels are a primary target of drugs (4, 5) and toxins found in animal venoms (6–8). As a result, Nav channel activity can be influenced by a variety of naturally occurring molecules, with the voltage sensors in all four domains representing the foremost target of tarantula toxins (9). The conventional view is that animal toxins interact with ion channel voltage sensors through direct protein–protein interactions (10–13). However, crystallographic and functional studies on voltage-activated potassium (Kv) channels have revealed an important role for the lipid membrane in regulating how Kv channels gate in response to changes in voltage (11–22). In addition, recent reports show that tarantula toxins can interact with Kv channel voltage sensors by partitioning into the membrane and binding to S3b-S4 paddle motifs at the protein–lipid interface (23–27). The discovery that several of these toxins also interact with paddle motifs found in Nav channels implies that partitioning can enable tarantula toxins to interact with voltage sensors in this family of ion channels as well (25, 28). Therefore, an emerging concept in the ion channel field is that the toxin pharmacology of an ion channel is not only determined by ligand–protein interactions, but also by the lipids in the surrounding membrane.

Cysteine palmitoylation is a common reversible lipid modification and has been shown to control cell surface expression, spatial organization, protein–protein interactions, and functional properties of a range of membrane proteins (29–35). Consequently, dysregulation of this process in human physiology is thought to play a key role in schizophrenia, mental retardation, Huntington's disease, and cancer (36–41). In rat brain neurons, palmitoylation is required for the biosynthesis and processing of Nav channels as they traffic to the membrane (42). However, little is known about the influence of this lipid modification on the functional properties of Nav channels. Furthermore, the notion that this posttranslational modification can affect the pharmacological properties of Nav channels has not been explored.

While surveying the animal toxin susceptibility of various Nav channel isoforms, we came across a mutant of rNav1.2a (43) that exhibits a higher apparent affinity for the tarantula toxin PaurTx3 (44) compared with the wild-type (wt) channel. Interestingly, the amino acid responsible for this discrepancy in toxin sensitivity was identified as a cysteine and is located in an intracellular loop of the channel, a region unlikely to be directly accessible to peptide toxins applied to the external solution. To explore whether cysteine palmitoylation is responsible for the altered pharmacological properties of the mutant, we removed intracellularly attached palmitate molecules from both wt and mutant channels and investigated changes in the sensitivity to a range of tarantula and scorpion toxins. The results from our experiments suggest that palmitoylation not only plays an important role in fine-tuning the extracellular pharmacological properties of wt rNav1.2a, but also that this protein modification can affect the gating properties of the channel.

Results

Intracellular Mutation Affects rNav1.2a Toxin Pharmacology. The tarantula toxin PaurTx3 potently inhibits wt rNav1.2a activation by interacting with the voltage sensor in domain II (28, 44). Here, we report a mutant of rNav1.2a with an increased sensitivity to PaurTx3 compared with the wt channel. Plotting the concentration dependence for toxin inhibition as fraction unbound measured at negative voltages (Fu; *Materials and Methods*) reveals that the mutant channel is ≈20-fold more susceptible to PaurTx3 than rNav1.2a itself (Fig. 1 *A* and *B* and Fig. S1*A*): The apparent affinity of the toxin for the wt channel is ≈27 nM, whereas toxin affinity for the mutant channel is ≈1 nM (Tables S1 and S2). The amino acid difference responsible for this discrepancy in toxin sensitivity was identified as a glycine to cysteine mutation at position 1079 (G1079C; Fig. S1*B*) located in the intracellular loop between domain II and domain III of the channel. In addition to altering the pharmacological properties of rNav1.2a, the cysteine substitution causes the channel to activate at more negative voltages (≈9 mV), whereas other gating properties remain relatively unaltered (Fig. 1 *C* and *D* and Tables S1 and S2).

Author contributions: F.B., M.M., and K.J.S. designed research; F.B. and M.M. performed research; F.B. and M.M. analyzed data; and F.B. and K.J.S. wrote the paper.

The authors declare no conflict of interest.

This article is a PNAS Direct Submission.

[1]To whom correspondence may be addressed. E-mail: swartzk@ninds.nih.gov or bosmansf@ninds.nih.gov.

This article contains supporting information online at www.pnas.org/lookup/suppl/doi:10.1073/pnas.1108497108/-/DCSupplemental.

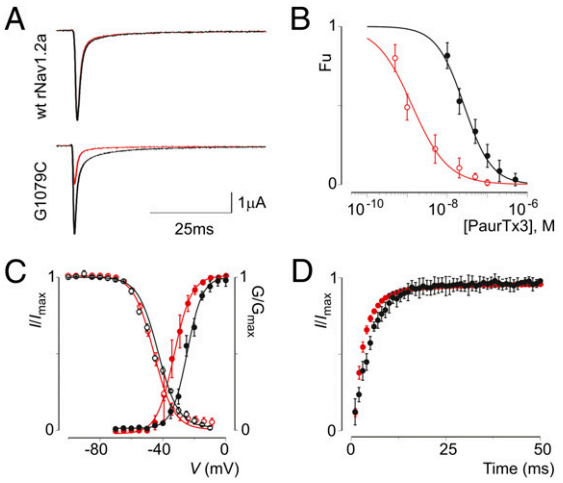

Fig. 1. Gating characteristics and sensitivity of wt rNav1.2a and G1079C to PaurTx3. (*A*) Effect of 10 nM PaurTx3 on wt rNav1.2a and the mutant channel. Sodium currents are elicited by a depolarization to 0 mV before (black) and after (red) addition of PaurTx3 from a holding potential of −90 mV. (*B*) Apparent affinity for PaurTx3 interacting with wt rNav1.2a (black) and the mutant channel (red). Concentration dependence for toxin inhibition plotted as fraction unbound (Fu) is shown. Lines represent a fit with the Hill equation; n = 3–5 for each toxin concentration and error bars represent SEM. (*C*) Normalized conductance–voltage and steady-state inactivation relationships of the wt rNav1.2a channel (black) and the G1079C mutation (red). (*D*) Recovery from fast inactivation of the wt channel (black) and mutant (red) determined by a double pulse protocol to 0 mV with a varying time between pulses (0–50 ms). Values are reported in Tables S1 and S2. n = 12, and error bars represent SEM.

To explore the extent to which the G1079C mutation alters Nav channel pharmacology, we compared the effects of a range of toxins on wt rNav1.2a and G1079C. In particular, we tested two tarantula toxins (ProTx-I and ProTx-II; ref. 45) that are thought to act through the membrane (25, 46) and two scorpion toxins [AaHII (47) and TsVII (48)] for which the membrane interaction is unclear (12, 46, 49). Each of these toxins target one or more of the voltage sensors in rNav1.2a, and collectively they interact with all four (12, 28, 50–54) (Fig. S2*A*). As is the case with PaurTx3, the apparent affinity of ProTx-II for the G1079C mutant is approximately eightfold higher than for the wt channel (Fig. S2*B* and Table S2). In contrast to PaurTx3 and ProTx-II, the susceptibility of both wt channel and G1079C for ProTx-I, TsVII, and AaHII are relatively unaltered (Fig. S2 *C–E* and Table S2).

Similar to other tarantula toxins (23–27, 46), PaurTx3 partitions into the membrane (Fig. S3), thereby raising the possibility that changes in the lipid membrane environment surrounding the targeted voltage sensor in domain II (28) can alter channel sensitivity for the toxin. Because the intracellular region containing the mutation is unlikely to be directly accessed by PaurTx3 or ProTx-II, we investigated whether intracellular cysteine modifications are responsible for the difference in toxin affinity between wt rNav1.2a and the G1079C mutant. Although a variety of lipids can be attached to a protein (55, 56), cysteine *S*-palmitoylation is one of the most common and reversible modifications that occur on the cytoplasmic side of the membrane (34). Therefore, we examined whether Nav channel palmitoylation underlies the increased susceptibility of the G1079C mutant for PaurTx3 and ProTx-II.

Chemical Inhibition of Palmitoylation Alters the Toxin Pharmacology of rNav1.2a. To explore whether palmitoylation can alter the pharmacological properties of mature Nav channels, we expressed both wt rNav1.2a and the G1079C mutant in *Xenopus* oocytes and incubated cells with 2-Br-palmitate, a nonmetabolizable palmitate analog thought to inhibit palmitate incorporation into proteins (57). Next, we compared the apparent affinity of PaurTx3 and ProTx-II for wt and G1079C channels before and after 2-Br-palmitate treatment. As a result, we found that depalmitoylating wt rNav1.2a increases the apparent affinity of PaurTx3 by approximately threefold, whereas the apparent affinity of the toxin for the G1079C mutant decreases approximately ninefold (Fig. 2*A* and Table S2), resulting in dose–response curves that coincide. Similar to PaurTx3, the apparent affinity of ProTx-II for wt rNav1.2a and G1079C coincides after 2-Br-palmitate treatment (Fig. 2*B* and Table S2). In contrast to PaurTx3 and ProTx-II, the apparent affinity of ProTx-I for wt rNav1.2a and G1079C does not change after removing palmitate molecules from the channels (Fig. S2*C* and Table S2). Altogether, these results suggest that the additional cysteine in the domain II-domain III loop of G1079C is palmitoylated and is responsible for the discrepancy in susceptibility of

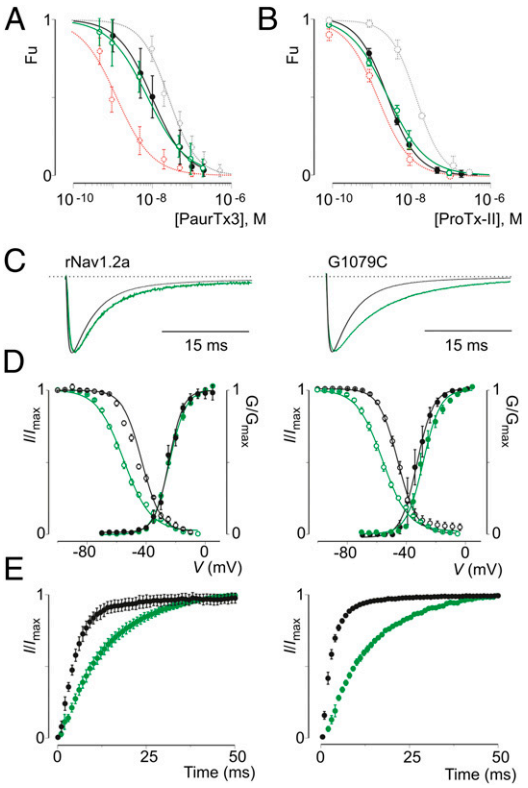

Fig. 2. Effects of palmitoylation on the pharmacology and function of wt rNav1.2a and G1079C. (*A*) Apparent affinity for PaurTx3 interacting with wt rNav1.2a (black) and the G1079C mutant (green) after channel depalmitoylation. Concentration dependence for toxin inhibition plotted as Fu measured at negative voltages is shown. Data are compared with that shown in Fig. 1*B*, which is represented in this figure by a dotted line and symbols. Solid lines represent a fit with the Hill equation. n = 3–5 for each toxin concentration, and error bars represent SEM. (*B*) Apparent affinity for ProTx-II interacting with wt rNav1.2a (black) and the G1079C mutant (green) after channel depalmitoylation. Data are compared with rNav1.2a (gray) and G1079C (red) before addition of 2-Br-palmitate. (*C*) Comparison of Nav channel fast inactivation before (black) and after (green) channel depalmitoylation for rNav1.2a (*Left*) and G1079C (*Right*). Nav channels were depolarized to −20 mV from a holding potential of −90 mV. (*D* and *E*) Side-by-side comparison of the effects of 2-Br-palmitate on the gating properties of rNav1.2a (*Left*) and G1079C (*Right*). *D* shows deduced conductance–voltage and steady-state inactivation relationships before (black) and after (green) depalmitoylation. *E* shows recovery from fast inactivation before (black) and after (green) depalmitoylation determined by a double pulse protocol to 0 mV with a varying time between pulses (0–50 ms). n = 3, and error bars represent SEM. Values are reported in Tables S1 and S2.

both channel variants for PaurTx3. Furthermore, our results reveal that intracellular palmitoylation can alter the susceptibility of wt rNav1.2a to PaurTx3 (threefold) and ProTx-II (fivefold). Interestingly, the G1079C mutation does not affect every toxin that interacts with the voltage sensors in rNav1.2a (Fig. S2 *C–E* and Table S2), suggesting that channel palmitoylation has a relatively local influence on how toxins interact with voltage sensors within the membrane.

Chemical Inhibition of Palmitoylation Alters the Gating Properties of rNav1.2a. Relatively few studies have reported effects of palmitoylation on the gating properties of voltage-activated ion channels. For example, the addition of a palmitate to a specific cysteine in the pore-forming subunit of Kv1.1 results in a 20-mV hyperpolarizing shift of the current–voltage relationship (58). Moreover, palmitoylation of auxiliary β-subunits has been shown to influence the gating properties of voltage-activated calcium channels (59–61) and epithelial sodium channels (62). Although it was demonstrated that [^{3}H] palmitate incorporates into the pore-forming subunit of wt rNav1.2a (42), it is unclear which cysteines are targeted. However, palmitoyl proteomics (63) and computational prediction of palmitoylation sites in rNav1.2a suggests several intracellular cysteines, including the one introduced by the G1079C mutation (64).

Removing palmitate molecules from intracellular cysteines with 2-Br-palmitate has two substantial effects on both wt rNav1.2a and G1079C gating (Fig. 2 *D* and *E* and Tables S1 and S2): (*i*) Steady-state inactivation is shifted toward more hyperpolarized voltages by ≈10 mV (Fig. 2*D*); and (*ii*) recovery from fast inactivation is approximtaely threefold slower (Fig. 2*E*). A more subtle outcome of 2-Br-palmitate treatment is that fast inactivation slows with G1079C being more sensitive than wt rNav1.2a (Fig. 2*C*). Taken together, these results suggest that palmitoylation influences the gating properties of wt rNav1.2a by altering the inactivation process, which may increase the pool of channels that are available for activation at resting membrane potentials (2). Intrigued by the modulatory effect of 2-Br-palmitate on channel function, we set out to identify endogenous cysteines that are capable of influencing the toxin pharmacology and gating properties of Nav channels through palmitoylation.

Intracellular Cysteines Can Influence the Pharmacological Properties of rNav1.2a. Even though the G1079C mutation was discovered serendipitously, it sparked our investigation into the functional consequences of rNav1.2a palmitoylation. To expand the relevance of the results obtained with this particular mutant, we searched for endogenous cysteines that affect the functional and pharmacological properties of wt rNav1.2a similar to 2-Br-palmitate treatment. To this end, we used a computational approach to predict palmitoylation of intracellular cysteines (64) and substituted three likely candidates with alanine (C650A in the domain I-II loop, and C1053A and C1182A in the domain II-III loop) (Fig. S2*A*). Next, we expressed the triple mutant (rNav1.2a^{AAA}) in *Xenopus* oocytes and compared its functional and pharmacological properties to wt rNav1.2a.

Strikingly, rNav1.2a^{AAA} displays the two distinct properties that are characteristic of chemically depalmitoylated wt rNav1.2a channels (Table S3): (*i*) Steady-state inactivation is shifted toward more hyperpolarized voltages (≈13 mV) (Fig. 3*B*); and (*ii*) recovery from fast inactivation is approximately twofold slower (Fig. 3*C*). In addition, we observe an increase in PaurTx3 sensitivity for the mutant rNav1.2a^{AAA} channel (Fig. 3*D* and Table S3), a feature similar to what we found for wt rNav1.2a channels treated with 2-Br-palmitate (Fig. 2*A*). A unique trait of rNav1.2a^{AAA} is that the channel activates at more negative voltages (≈11 mV), whereas 2-Br-palmitate treatment of wt rNav1.2a does not alter the activation voltage of the channel (Figs. 2*D* and Fig. 3*B* and Tables S1–S4). However, given the importance of the domain I-II and domain

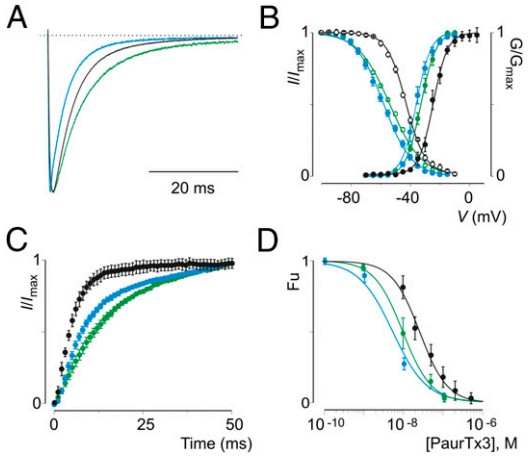

Fig. 3. Gating characteristics and PaurTx3 sensitivity of rNav1.2^{AAA}. (*A*) Comparison of Nav channel fast inactivation for wt rNav1.2a (black) and rNav1.2^{AAA} before (blue) or after (green) depalmitoylation with 2-Br-palmitate. Nav channels were depolarized to −20 mV from a holding potential of −90 mV. (*B* and *C*) Comparison of the gating properties of rNav1.2a (black) and rNav1.2^{AAA} before (blue) or after (green) depalmitoylation. *B* shows deduced conductance–voltage and steady-state inactivation relationships; *C* shows recovery from fast inactivation as determined by a double-pulse protocol to −20 mV with a varying time between pulses (0–50 ms). n = 3, and error bars represent SEM. (*D*) Apparent affinity of PaurTx3 for rNav1.2a (black) and rNav1.2^{AAA} before (blue), or after (green) depalmitoylation with 2-Br-palmitate. Concentration dependence for toxin inhibition plotted as Fu measured at negative voltages is shown. Solid lines represent a fit with the Hill equation. n = 3–5 for each toxin concentration, and error bars represent SEM. Values are reported in Tables S3 and S4.

II-III intracellular loops in Nav channel gating (65) and their interaction with auxiliary proteins (66, 67), one explanation for this observation may be that the substitution of a strategic cysteine itself alters the activation characteristics of rNav1.2a^{AAA}. In concert, 2-Br-palmitate treatment only marginally affects the gating characteristics (Fig. 3 *A–C* and Table S3) and PaurTx3 susceptibility (Fig. 3*D* and Table S4) of rNav1.2a^{AAA}, suggesting that the three cysteine substitutions have removed palmitate molecules that influence the gating and pharmacological properties of wt rNav1.2a. Additionally, these results support the value of 2-Br-palmitate as a chemical tool to specifically remove palmitate molecules from intracellular cysteines (68).

According to the prediction software that we used (64), C1182 is the most likely residue to be palmitoylated in wt rNav1.2a. We therefore constructed an additional rNav1.2a mutant in which we replaced this cysteine with an alanine and investigated its functional characteristics. Interestingly, C1182A largely mimics the hyperpolarizing effect of rNav1.2a^{AAA} on channel activation and steady-state inactivation (Fig. 4*A* and Table S3). Although recovery from fast inactivation slows down as well (Fig. 4*B* and Table S3), the effect is less pronounced compared with rNav1.2a^{AAA} (Fig. 3*C* and Table S3). Similar to the triple mutant, 2-Br-palmitate treatment only has a subtle additional effect on the activation and steady-state inactivation properties of C1182A (Fig. 4*A* and Table S3). In contrast, recovery from fast inactivation slows down further after treatment (Fig. 4*B* and Table S3), suggesting that palmitoylation of C650, C1053, or other intracellular cysteines may play a role in this aspect of gating. Further support for the involvement of C1182 in channel palmitoylation comes from toxin experiments in which we observe an augmented susceptibility of the C1182A mutant for PaurTx3. As with rNav1.2a^{AAA}, the resulting apparent affinity of the toxin for C1182A is identical to that obtained with depalmitoylated wt rNav1.2a channels and is only slightly influenced by 2-Br-palmitate treatment (Figs. 2*A* and

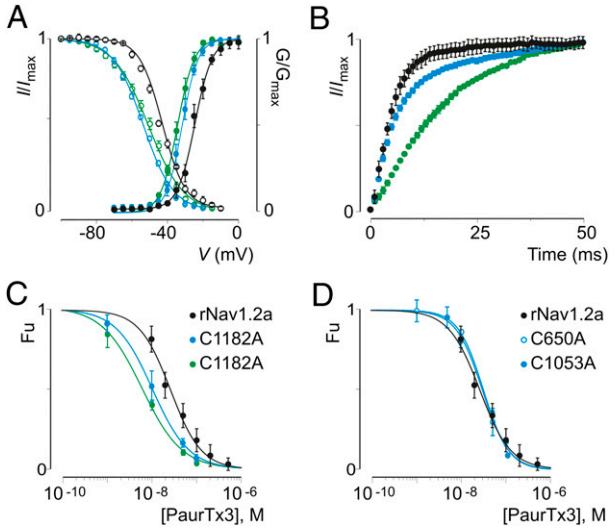

Fig. 4. Gating characteristics and PaurTx3 sensitivity of C1182A. (*A* and *B*) Comparison of the gating properties of rNav1.2a (black) and C1182A before (blue) or after (green) depalmitoylation with 2-Br-palmitate. *A* shows deduced conductance–voltage and steady-state inactivation relationships; *B* shows recovery from fast inactivation as determined by a double-pulse protocol to −20 mV with a varying time between pulses (0–50 ms). n = 3–5, and error bars represent SEM. (*C*) Apparent affinity of PaurTx3 for rNav1.2a (black) and C1182A before (blue) or after (green) depalmitoylation. (*D*) Apparent affinity of PaurTx3 for rNav1.2a (black), C650A (blue, open circles), and C1053A (blue, filled circles). n = 3–4 for each toxin concentration, and error bars represent SEM. Values are reported in Tables S3 and S4.

4*C* and Tables S1–S4). To check whether other intracellular cysteines are important in toxin pharmacology, we constructed the individual C650A and C1053A mutants but detected no change in the apparent affinity of PaurTx3 for these channel mutants (31 ± 2 nM and 30 ± 3 nM, respectively) (Fig. 4*D*), suggesting that palmitoylation of C1182 is largely responsible for the decrease in sensitivity of wt rNav1.2a for PaurTx3.

Taken together, our results with rNav1.2a^{AAA} and the C1182A mutant identify potential palmitoylation sites within the channel and suggest that palmitoylation of cysteines in the wt rNav1.2a channel can alter the gating properties and pharmacological sensitivities of the channel.

Cholesterol Influences the Toxin Pharmacology of rNav1.2a. Palmitoylation is thought to play an important role in targeting membrane proteins to detergent-resistant membrane fractions, or lipid microdomains (55). Therefore, we wanted to investigate whether this phenomenon could be responsible for the influence of intracellular palmitate molecules on tarantula toxin susceptibility of rNav1.2a. We used a commonly used approach to break up lipid microdomains (69) and studied whether the effects on toxin pharmacology were similar as observed after channel depalmitoylation. To this end, we incubated Nav channel-expressing *Xenopus* oocytes with methyl-β-cyclodextrin and measured the apparent affinity of PaurTx3. Compared with 2-Br-palmitate (Fig. 2 *C–E* and Table S1), the effects of removing cholesterol from the membrane on the gating properties of wt rNav1.2a are relatively subtle (Fig. 5*A*). Surprisingly, however, cholesterol depletion decreases the apparent affinity of PaurTx3 for wt rNav1.2a by a factor of 10 (from 27 ± 10 nM to 289 ± 37 nM; Fig. 5*B*), whereas depalmitoylating the channel has the opposite effect on toxin affinity (Fig. 2*A* and Table S2). In contrast to wt rNav1.2a, cholesterol depletion causes the mutant that sparked this investigation, G1079C, to activate at more-positive voltages (≈7 mV) (Fig. S4). Moreover, the apparent affinity of PaurTx3 for G1079C decreases ≈25-fold (from 1 ± 1 nM to 26 ± 2 nM; see Fig. 5*C*) after cholesterol depletion, an effect that is also observed when the mutant channel is treated with 2-Br-palmitate (Fig. 2*A* and Table S2). In concert with the results obtained after 2-Br-palmitate treatment (Fig. S2*A* and Table S2), the interaction of ProTx-I with wt rNav1.2a and G1079C is not influenced by cholesterol depletion (Fig. S4*B*).

Overall, these results show that palmitoylation and cholesterol influence the pharmacological properties of rNav1.2a. For the G1079C mutant in particular, the similar effects on toxin affinity after 2-Br-palmitate and methyl-β-cyclodextrin treatment would be consistent with this channel variant being targeted to specific lipid microdomains that alter its susceptibility to PaurTx3 (70).

Discussion

Although it was shown before that the incorporation of palmitate molecules is a critical step in the biosynthesis of Nav channels (42), the advent of more precise tools such as 2-Br-palmitate (57) allows us to examine the role of palmitoylation in Nav channel function and pharmacology more closely. Together with site-directed mutagenesis, we used 2-Br-palmitate to test our hypothesis that palmitoylation of an introduced cysteine in the intracellular loop between domains II and III of rNav1.2a (G1079C) is responsible for a 20-fold increase in apparent affinity for PaurTx3 (Fig. 1*A* and *B* and Table S2), a peptide toxin isolated from tarantula venom (44) that interacts with the domain II voltage sensor in wt rNav1.2a (28). As a result, we revealed an important role for palmitoylation in shaping the functional properties of wt rNav1.2a because 2-Br-palmitate treatment of the channel significantly alters its gating characteristics (Fig. 2 *C–E* and Table S1). Furthermore, depalmitoylation causes the gating properties of G1079C and the wt channel to coincide and abolishes the disparity in apparent affinity of PaurTx3 (Fig. 2*A* and Tables S1 and S2), suggesting that the additional cysteine in G1079C is palmitoylated and that this lipid modification is responsible for the increase in apparent affinity of PaurTx3. Moreover, we identified endogenous palmitoylation sites in wt rNav1.2a that can modulate channel function and toxin pharmacology. In particular, we constructed a triple cysteine mu-

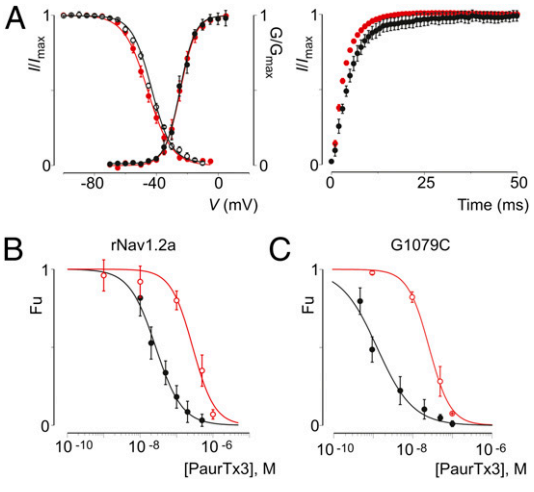

Fig. 5. Effects of cholesterol on PaurTx3 interaction with wt rNav1.2a and G1079C. (*A*) Effects of cholesterol depletion on the gating properties of rNav1.2a; deduced conductance–voltage and steady-state inactivation relationships (*Left*) and recovery from fast inactivation (*Right*) before (black) and after (red) 5 mM methyl-β-cyclodextrin are shown. n = 3, and error bars represent SEM. (*B* and *C*) Apparent affinity of PaurTx3 interacting with rNav1.2a (*B*) and G1079C (*C*) before (black) and after (red) membrane cholesterol depletion. Solid line represents a fit with the Hill equation, and error bars represent SEM.

tant (rNav1.2a^{AAA}) with an increased susceptibility for PaurTx3 and a gating behavior strongly reminiscent of wt rNav1.2a channels treated with 2-Br-palmitate (Fig. 3 and Tables S3 and S4). Palmitoylation of one cysteine in particular (C1182) primarily influences PaurTx3 sensitivity (Fig. 4*C* and Table S4) and may alter the inactivation process of rNav1.2a in neurons thereby potentially increasing the pool of neuronal channels that are more readily available for activation.

Because it is rather remarkable that intracellular mutations can alter the sensitivity of rNav1.2a to extracellular peptide ligands, it is interesting to consider the underlying mechanisms. On a macroscopic level, palmitoylation is thought to target proteins to lipid microdomains within the membrane (55). As such, changes in the palmitoylation pattern of rNav1.2a may redirect the channel to a region with a particular lipid composition and a predisposition to attract specific toxins that partition in the membrane before interacting with the channel. Although PaurTx3 (Fig. S3) and ProTx-II (46) have been shown to partition into membranes, so has ProTx-I (25), yet the apparent affinity of ProTx-I is not affected by the G1079C mutation and the membrane lipid modifications tested in this study (Figs. S2*C* and S4*B*). Therefore, additional toxin interactions with specific rNav1.2a voltage sensors may play a role as well. Structural studies on Kv channels and bacterial Nav channels have shown that the voltage sensor of one subunit is positioned adjacent to the pore-forming helices of the next subunit (Fig. S2*A*) (14–16, 22, 71). Because of their sequence similarity with these channels, it is likely that mammalian Nav channels share a similar structural organization. Given the location of the C1182A and G1079C mutation in the intracellular loop between domains II and III (Fig. S2*A*), one could imagine that toxins targeting the voltage sensor in domain II (28, 50, 53) would be susceptible to the presence of a palmitate molecule in this region. Although all toxins affected by palmitoylation interact with the voltage sensor in domain II (Fig. 2 *A* and *B*, Fig. S2 *A* and *B*, and Tables S1 and S2), not all domain II toxins are affected by the lipid modification (Fig. S2 *A, C,* and *D*), suggesting that sensitivity to palmitoylation is not exclusively determined by the voltage sensor it targets, but by the local interactions between a specific toxin and voltage sensor within the membrane. Further investigation should be performed to determine the mechanisms by which palmitoylation influences Nav channel gating and pharmacology, and to explore whether similar regulatory mechanisms occur for other membrane proteins (35).

Materials and Methods

Spider and Scorpion Toxin Purification. PaurTx3 was purified from *Phrixotrichus* auratus venom (Spider Pharm) by using a two-step HPLC protocol (28, 50, 53). Identity and purity were determined with mass spectrometry and automated peptide sequencing. AaHII from *Androctonus australis* hector venom and TsVII from *Tityus serrulatus* venom were purified as described (47, 48), and synthetic ProTx-I and ProTx-II were acquired from Peptides International. Toxins were kept at −20 °C. Before experiments, toxin aliquots were dissolved in appropriate solutions containing 0.1% BSA.

Two-Electrode Voltage-Clamp Recording from *Xenopus* Oocytes. The DNA sequence of rNav1.2a, rNav1.2a^{AAA}, C650A, C1053A, C1182A, and G1079C was confirmed by automated DNA sequencing and cRNA was synthesized by using T7 polymerase (mMessage mMachine kit; Ambion) after linearizing the DNA with appropriate restriction enzymes. Channels were expressed in *Xenopus* oocytes and studied after 1–2 d of incubation after cRNA injection (incubated at 17 °C in 96 mM NaCl, 2 mM KCl, 5 mM Hepes, 1 mM $MgCl_2$, 1.8 mM $CaCl_2$, and 50 μg/mL gentamycin at pH 7.6 with NaOH) using two-electrode voltage-clamp recording techniques (OC-725C; Warner Instruments) with a 150-μL recording chamber. Data were filtered at 3 kHz and digitized at 20 kHz by using pClamp software (Axon). Microelectrode resistances were 0.1–1 MΩ when filled with 3 M KCl. The external recording solution (ND96) contained 96 mM NaCl, 2 mM KCl, 5 mM Hepes, 1 mM $MgCl_2$, and 1.8 mM $CaCl_2$ at pH 7.6 with NaOH. All experiments were performed at room temperature (≈22 °C). Protein palmitoylation was inhibited by using a previously reported procedure consisting of overnight incubation of oocytes with 100 μM 2-Br-palmitate and rinsed in ND96 before recording (57, 68). Oocytes were exposed to 5 mM methyl-β-cyclodextrin for ≥2 h to extract cholesterol from the membrane (69) and rinsed in ND96 before recording. Leak and background conductances, identified by blocking the channel with tetrodotoxin, have been subtracted for all Nav channel currents.

Analysis of Channel Activity and Toxin–Channel Interactions. Voltage–activation relationships were obtained by measuring steady-state currents and calculating conductance (G), and a single Boltzmann function was fitted to the data according to: $G/G_{max} = (1 + e^{-zF(V - V_{1/2})/RT})^{-1}$ where G/G_{max} is the normalized conductance, z is the equivalent charge, $V_{1/2}$ is the half-activation voltage, F is Faraday's constant, R is the gas constant, and T is temperature in Kelvin. Occupancy of closed or resting channels by toxins was examined by using negative holding voltages where open probability was very low, and the fraction of unbound channels (Fu) was estimated by using depolarizations that are too weak to open toxin-bound channels, as described (28). After addition of the toxin to the recording chamber, the equilibration between the toxin and the channel was monitored by using weak depolarizations elicited at 5- to 10-s intervals. For both wt and mutant channels, we recorded G–V relationships in the absence and presence of toxin. Concentration dependence for toxin inhibition of Nav channels is plotted as Fu measured at negative voltages versus concentration. The Hill equation was used to fit the data and to obtain apparent affinity values. α-Scorpion toxin affinity was determined as described by measuring the $I_{10\ ms}/I_{peak}$ ratio which gives an estimate of the probability for the channels not to be inactivated after 10 ms (72). Off-line data analysis was performed by using Clampfit (Axon), and Origin 7.5 (Originlab).

ACKNOWLEDGMENTS. We thank Al Goldin for the rNav1.2a clone and Marie-France Martin-Eauclaire for AaHII and TsVII; the National Institute of Neurological Disorders and Stroke protein sequencing facility; and the members of the K.J.S., Holmgren, Mindell, and Mayer laboratories for discussions.

1. Bean BP (2007) The action potential in mammalian central neurons. *Nat Rev Neurosci* 8:451–465.
2. Hille B (2001) *Ion Channels of Excitable Membranes* (Sinauer, Sunderland, MA), 3rd ed, p 814.
3. Bezanilla F (2000) The voltage sensor in voltage-dependent ion channels. *Physiol Rev* 80:555–592.
4. Catterall WA, Goldin AL, Waxman SG (2005) International Union of Pharmacology. XLVII. Nomenclature and structure-function relationships of voltage-gated sodium channels. *Pharmacol Rev* 57:397–409.
5. Kaczorowski GJ, McManus OB, Priest BT, Garcia ML (2008) Ion channels as drug targets: The next GPCRs. *J Gen Physiol* 131:399–405.
6. Catterall WA, et al. (2007) Voltage-gated ion channels and gating modifier toxins. *Toxicon* 49:124–141.
7. Terlau H, Olivera BM (2004) Conus venoms: A rich source of novel ion channel-targeted peptides. *Physiol Rev* 84:41–68.
8. Rodríguez de la Vega RC, Possani LD (2005) Overview of scorpion toxins specific for Na + channels and related peptides: Biodiversity, structure-function relationships and evolution. *Toxicon* 46:831–844.
9. Bosmans F, Swartz KJ (2010) Targeting voltage sensors in sodium channels with spider toxins. *Trends Pharmacol Sci* 31:175–182.
10. Cestèle S, et al. (1998) Voltage sensor-trapping: Enhanced activation of sodium channels by beta-scorpion toxin bound to the S3-S4 loop in domain II. *Neuron* 21: 919–931.
11. Li-Smerin Y, Swartz KJ (2000) Localization and molecular determinants of the Hanatoxin receptors on the voltage-sensing domains of a K(+) channel. *J Gen Physiol* 115:673–684.
12. Rogers JC, Qu Y, Tanada TN, Scheuer T, Catterall WA (1996) Molecular determinants of high affinity binding of alpha-scorpion toxin and sea anemone toxin in the S3-S4 extracellular loop in domain IV of the Na+ channel alpha subunit. *J Biol Chem* 271: 15950–15962.
13. Swartz KJ, MacKinnon R (1997) Mapping the receptor site for hanatoxin, a gating modifier of voltage-dependent K+ channels. *Neuron* 18:675–682.
14. Jiang Y, et al. (2003) X-ray structure of a voltage-dependent K+ channel. *Nature* 423: 33–41.
15. Jiang Y, Ruta V, Chen J, Lee A, MacKinnon R (2003) The principle of gating charge movement in a voltage-dependent K+ channel. *Nature* 423:42–48.
16. Long SB, Tao X, Campbell EB, MacKinnon R (2007) Atomic structure of a voltage-dependent K+ channel in a lipid membrane-like environment. *Nature* 450:376–382.
17. Ramu Y, Xu Y, Lu Z (2006) Enzymatic activation of voltage-gated potassium channels. *Nature* 442:696–699.
18. Schmidt D, Cross SR, MacKinnon R (2009) A gating model for the archeal voltage-dependent K(+) channel KvAP in DPhPC and POPE:POPG decane lipid bilayers. *J Mol Biol* 390:902–912.
19. Schmidt D, Jiang QX, MacKinnon R (2006) Phospholipids and the origin of cationic gating charges in voltage sensors. *Nature* 444:775–779.

20. Schmidt D, MacKinnon R (2008) Voltage-dependent K+ channel gating and voltage sensor toxin sensitivity depend on the mechanical state of the lipid membrane. *Proc Natl Acad Sci USA* 105:19276–19281.
21. Xu Y, Ramu Y, Lu Z (2008) Removal of phospho-head groups of membrane lipids immobilizes voltage sensors of K+ channels. *Nature* 451:826–829.
22. Chakrapani S, Cuello LG, Cortes DM, Perozo E (2008) Structural dynamics of an isolated voltage-sensor domain in a lipid bilayer. *Structure* 16:398–409.
23. Jung HJ, et al. (2005) Solution structure and lipid membrane partitioning of VSTx1, an inhibitor of the KvAP potassium channel. *Biochemistry* 44:6015–6023.
24. Lee SY, MacKinnon R (2004) A membrane-access mechanism of ion channel inhibition by voltage sensor toxins from spider venom. *Nature* 430:232–235.
25. Milescu M, et al. (2009) Interactions between lipids and voltage sensor paddles detected with tarantula toxins. *Nat Struct Mol Biol* 16:1080–1085.
26. Milescu M, et al. (2007) Tarantula toxins interact with voltage sensors within lipid membranes. *J Gen Physiol* 130:497–511.
27. Phillips LR, et al. (2005) Voltage-sensor activation with a tarantula toxin as cargo. *Nature* 436:857–860.
28. Bosmans F, Martin-Eauclaire MF, Swartz KJ (2008) Deconstructing voltage sensor function and pharmacology in sodium channels. *Nature* 456:202–208.
29. Charollais J, Van Der Goot FG (2009) Palmitoylation of membrane proteins (Review). *Mol Membr Biol* 26:55–66.
30. Fukata Y, Fukata M (2010) Protein palmitoylation in neuronal development and synaptic plasticity. *Nat Rev Neurosci* 11:161–175.
31. Resh MD (2006) Palmitoylation of ligands, receptors, and intracellular signaling molecules. *Sci STKE* 2006:re14.
32. Hayashi T, Thomas GM, Huganir RL (2009) Dual palmitoylation of NR2 subunits regulates NMDA receptor trafficking. *Neuron* 64:213–226.
33. Shipston MJ (2011) Ion channel regulation by protein palmitoylation. *J Biol Chem* 286: 8709–8716.
34. Iwanaga T, Tsutsumi R, Noritake J, Fukata Y, Fukata M (2009) Dynamic protein palmitoylation in cellular signaling. *Prog Lipid Res* 48:117–127.
35. Macdonald-Obermann JL, Pike LJ (2009) Palmitoylation of the EGF receptor impairs signal transduction and abolishes high-affinity ligand binding. *Biochemistry* 48: 2505–2513.
36. Kim SJ, et al. (2008) Palmitoyl protein thioesterase-1 deficiency impairs synaptic vesicle recycling at nerve terminals, contributing to neuropathology in humans and mice. *J Clin Invest* 118:3075–3086.
37. Mukai J, et al. (2008) Palmitoylation-dependent neurodevelopmental deficits in a mouse model of 22q11 microdeletion. *Nat Neurosci* 11:1302–1310.
38. Oyama T, et al. (2000) Isolation of a novel gene on 8p21.3-22 whose expression is reduced significantly in human colorectal cancers with liver metastasis. *Genes Chromosomes Cancer* 29:9–15.
39. Raymond FL, et al. (2007) Mutations in ZDHHC9, which encodes a palmitoyltransferase of NRAS and HRAS, cause X-linked mental retardation associated with a Marfanoid habitus. *Am J Hum Genet* 80:982–987.
40. Zhang Z, et al. (2006) Palmitoyl-protein thioesterase-1 deficiency mediates the activation of the unfolded protein response and neuronal apoptosis in INCL. *Hum Mol Genet* 15:337–346.
41. Huang K, et al. (2010) Palmitoylation and function of glial glutamate transporter-1 is reduced in the YAC128 mouse model of Huntington disease. *Neurobiol Dis* 40: 207–215.
42. Schmidt JW, Catterall WA (1987) Palmitylation, sulfation, and glycosylation of the alpha subunit of the sodium channel. Role of post-translational modifications in channel assembly. *J Biol Chem* 262:13713–13723.
43. Auld VJ, et al. (1988) A rat brain Na+ channel alpha subunit with novel gating properties. *Neuron* 1:449–461.
44. Bosmans F, et al. (2006) Four novel tarantula toxins as selective modulators of voltage-gated sodium channel subtypes. *Mol Pharmacol* 69:419–429.
45. Middleton RE, et al. (2002) Two tarantula peptides inhibit activation of multiple sodium channels. *Biochemistry* 41:14734–14747.
46. Smith JJ, Alphy S, Seibert AL, Blumenthal KM (2005) Differential phospholipid binding by site 3 and site 4 toxins. Implications for structural variability between voltage-sensitive sodium channel domains. *J Biol Chem* 280:11127–11133.
47. Martin MF, Rochat H, Marchot P, Bougis PE (1987) Use of high performance liquid chromatography to demonstrate quantitative variation in components of venom from the scorpion Androctonus australis Hector. *Toxicon* 25:569–573.
48. Céard B, De Lima ME, Bougis PE, Martin-Eauclaire MF (1992) Purification of the main beta-toxin from Tityus serrulatus scorpion venom using high-performance liquid chromatography. *Toxicon* 30:105–110.
49. Cohen L, et al. (2006) Direct evidence that receptor site-4 of sodium channel gating modifiers is not dipped in the phospholipid bilayer of neuronal membranes. *J Biol Chem* 281:20673–20679.
50. Marcotte P, Chen LQ, Kallen RG, Chahine M (1997) Effects of Tityus serrulatus scorpion toxin gamma on voltage-gated Na+ channels. *Circ Res* 80:363–369.
51. Edgerton GB, Blumenthal KM, Hanck DA (2008) Evidence for multiple effects of ProTxII on activation gating in Na(V)1.5. *Toxicon* 52:489–500.
52. Smith JJ, Cummins TR, Alphy S, Blumenthal KM (2007) Molecular interactions of the gating modifier toxin ProTx-II with NaV 1.5: Implied existence of a novel toxin binding site coupled to activation. *J Biol Chem* 282:12687–12697.
53. Sokolov S, Kraus RL, Scheuer T, Catterall WA (2008) Inhibition of sodium channel gating by trapping the domain II voltage sensor with protoxin II. *Mol Pharmacol* 73: 1020–1028.
54. Xiao Y, Blumenthal K, Jackson, JO, 2nd, Liang S, Cummins TR (2010) The tarantula toxins ProTx-II and huwentoxin-IV differentially interact with human Nav1.7 voltage sensors to inhibit channel activation and inactivation. *Mol Pharmacol* 78:1124–1134.
55. Levental I, Grzybek M, Simons K (2010) Greasing their way: Lipid modifications determine protein association with membrane rafts. *Biochemistry* 49:6305–6316.
56. Nadolski MJ, Linder ME (2007) Protein lipidation. *FEBS J* 274:5202–5210.
57. Webb Y, Hermida-Matsumoto L, Resh MD (2000) Inhibition of protein palmitoylation, raft localization, and T cell signaling by 2-bromopalmitate and polyunsaturated fatty acids. *J Biol Chem* 275:261–270.
58. Gubitosi-Klug RA, Mancuso DJ, Gross RW (2005) The human Kv1.1 channel is palmitoylated, modulating voltage sensing: Identification of a palmitoylation consensus sequence. *Proc Natl Acad Sci USA* 102:5964–5968.
59. Mitra-Ganguli T, Vitko I, Perez-Reyes E, Rittenhouse AR (2009) Orientation of palmitoylated CaVbeta2a relative to CaV2.2 is critical for slow pathway modulation of N-type Ca2+ current by tachykinin receptor activation. *J Gen Physiol* 134:385–396.
60. Qin N, et al. (1998) Unique regulatory properties of the type 2a Ca2+ channel beta subunit caused by palmitoylation. *Proc Natl Acad Sci USA* 95:4690–4695.
61. Stephens GJ, Page KM, Bogdanov Y, Dolphin AC (2000) The alpha1B Ca2+ channel amino terminus contributes determinants for beta subunit-mediated voltage-dependent inactivation properties. *J Physiol* 525:377–390.
62. Mueller GM, et al. (2010) Cys palmitoylation of the beta subunit modulates gating of the epithelial sodium channel. *J Biol Chem* 285:30453–30462.
63. Kang R, et al. (2008) Neural palmitoyl-proteomics reveals dynamic synaptic palmitoylation. *Nature* 456:904–909.
64. Ren J, et al. (2008) CSS-Palm 2.0: An updated software for palmitoylation sites prediction. *Protein Eng Des Sel* 21:639–644.
65. Bennett ES (2004) Channel activation voltage alone is directly altered in an isoform-specific manner by Na(v1.4) and Na(v1.5) cytoplasmic linkers. *J Membr Biol* 197: 155–168.
66. Bouzidi M, et al. (2002) Interaction of the Nav1.2a subunit of the voltage-dependent sodium channel with nodal ankyrinG. In vitro mapping of the interacting domains and association in synaptosomes. *J Biol Chem* 277:28996–29004.
67. Fache MP, et al. (2004) Endocytotic elimination and domain-selective tethering constitute a potential mechanism of protein segregation at the axonal initial segment. *J Cell Biol* 166:571–578.
68. Resh MD (2006) Use of analogs and inhibitors to study the functional significance of protein palmitoylation. *Methods* 40:191–197.
69. Christian AE, Haynes MP, Phillips MC, Rothblat GH (1997) Use of cyclodextrins for manipulating cellular cholesterol content. *J Lipid Res* 38:2264–2272.
70. Dart C (2010) Lipid microdomains and the regulation of ion channel function. *J Physiol* 588:3169–3178.
71. Payandeh J, Scheuer T, Zheng N, Catterall WA (2011) The crystal structure of a voltage-gated sodium channel. *Nature* 475:353–358.
72. Chen H, et al. (2002) Differential sensitivity of sodium channels from the central and peripheral nervous system to the scorpion toxins Lqh-2 and Lqh-3. *Eur J Neurosci* 16: 767–770.